RSC Advances

PAPER

View Article Online
View Journal | View Issue

Cite this: *RSC Adv.*, 2020, **10**, 34006

Synthesis and properties of DNA oligomers containing stereopure phosphorothioate linkages and C-5 modified deoxyuridine derivatives†

Rintaro Iwata Hara,[ab] Reijiro Yoshino,[a] Yohei Nukaga,[a] Yusuke Maeda,[a] Kazuki Sato[a] and Takeshi Wada *[a]

Received 12th June 2020
Accepted 3rd September 2020

DOI: 10.1039/d0ra06970a

rsc.li/rsc-advances

Phosphorothioate (PS) modification, where a non-bridging oxygen atom in a phosphodiester linkage is replaced by a sulfur atom, is widely used to improve the properties of nucleic acid drugs. Each PS linkage can be found in two stereoisomers, *Rp* and *Sp*. Since one non-bridging oxygen or sulfur atom in *Sp*-PS or *Rp*-PS, respectively, is located close to the C-5 substituent of uracil in a DNA/RNA hybrid duplex, the combination of the stereochemistry of the PS linkages and the type of the C-5 modification of uracil bases is expected to affect the properties of the hybrid duplexes. Herein, DNA oligomers containing both stereopure phosphorohioate linkages and C-5 modified deoxyuridine derivatives were synthesized. The thermodynamic stability of the DNA/RNA and DNA/DNA duplexes and RNase H activity of the DNA/RNA duplexes were evaluated. The combination of 5-propynyluracil and (*Rp*)-PS linkages in a DNA strand could significantly increase the thermal stability of a DNA/RNA hybrid duplex without reducing its RNase H activity.

Introduction

Nucleic acid therapeutics, namely drugs based on nucleic acid molecules, such as DNA, RNA, and their derivatives, have been an attractive field for drug development for several decades. Nucleic acid drugs are classified into various categories, including antisense oligonucleotides (ASOs), small interfering RNAs (siRNAs), and aptamers. Particularly, the recent progress in ASOs has been so impressive that an increasing number of ASOs have been approved as therapeutics since 2010.[1]

ASOs are classified into two types, the ribonuclease H (RNase H)-dependent and the RNase H-independent ASOs, according to their mechanism of action after the duplex formation.[2] Although both types of ASOs bind to a complementary region of the target RNA, *e.g.*, mRNA, to form an ASO/RNA hybrid duplex, the RNase H-dependent ASOs induce the cleavage of the target RNAs by RNase H after the formation of the hybrid duplex. The RNase H-dependent ASOs contain several consecutive DNA regions and RNase H can recognize the DNA/RNA hybrid duplex structures in the ASO/RNA hybrid, thus cleaving the RNA strand.[2–5] In contrast, the RNase H-independent ASOs bind to the target RNA without cleaving the target RNA, but they sterically block some biological processes by the duplex formation.

Since nucleic acid molecules are susceptible to cleavage by endogenous nucleases *in vivo*, their chemical modification is essential for therapeutic application. Among them, phosphorothioate (PS) modification, where a non-bridging oxygen atom in a phosphodiester linkage is replaced by a sulfur atom, is the most employed modification for P-atoms. PS modification improves the properties of ASOs, including nuclease stability and pharmacokinetics,[2,6] and has already been adopted for the development of several ASO drugs. Although the PS modification seems to be established for the chemical modification of ASOs, it should be noted that the P-atom in PS linkages is chiral different from that in phosphodiester (PO)-linkages, and the (*Rp*)-PS and (*Sp*)-PS diastereomers exhibit completely different physicochemical and biological properties (Fig. 1).[7–12]

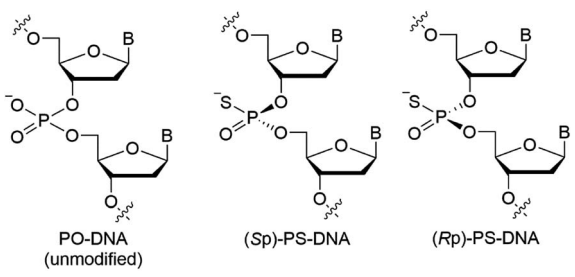

Fig. 1 Structures of PO-DNA and the two stereoisomers of PS-DNA.

[a]*Faculty of Pharmaceutical Sciences, Tokyo University of Science, 2641 Yamazaki, Noda, Chiba 278-8510, Japan. E-mail: twada@rs.tus.ac.jp*

[b]*Department of Neurology and Neurological Science, Graduate School of Medical and Dental Sciences, Tokyo Medical and Dental University, 1-5-45, Yushima, Bunkyo-Ku, Tokyo, 113-8519, Japan*

† Electronic supplementary information (ESI) available. See DOI: 10.1039/d0ra06970a

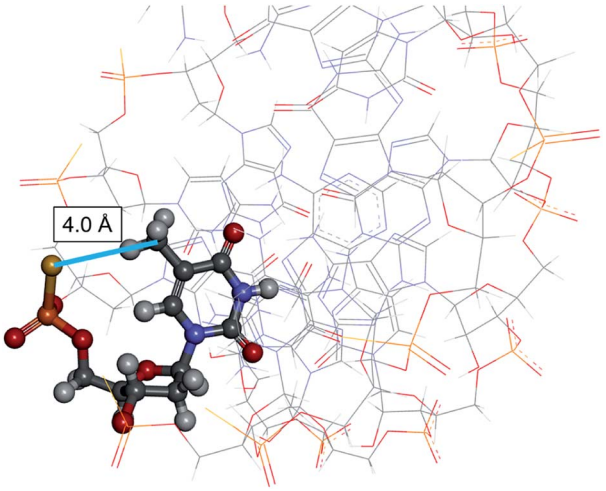

Fig. 2 3D view of an *R*p-PS-DNA/RNA hybrid duplex, all-(*R*p)-dG$_{PS}$C$_{PS}$G$_{PS}$T$_{PS}$C$_{PS}$A$_{PS}$G$_{PS}$G/rCCUGACGC (PDB 8PSH, NMR solution structure).[13] The underlined $\underline{_{PS}T}$ residue is displayed in ball-and-stick style. The distance between the carbon atom of the methyl group of thymine and the sulfur atom in the *R*p-PS linkage was 4.0 Å.

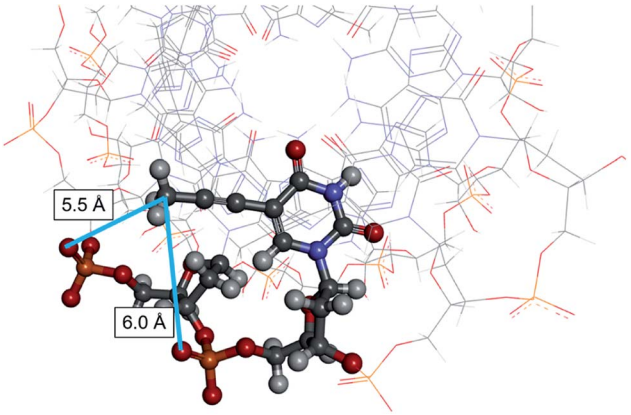

Fig. 4 3D view of the ^{pr}U-contained-DNA/RNA hybrid duplex, dG^{pr}C^{pr}U^{pr}U^{pr}C^{pr}U^{pr}C^{pr}U ^{pr}UC/rGAAGAGAAGC[28] (PDB 1OO7, NMR solution structure). The underlined ^{pr}U residue and two phosphate groups close to the methyl group of the ^{pr}U are displayed in ball-and-stick style. The distance between the carbon atom of the methyl group of ^{pr}U and the sulfur atom in a pro-*R*p oxygen atom in a phosphodiester linkage was 5.5 Å, and the distance between the same carbon atom and another pro-*R*p oxygen atom was 6.0 Å.

In an ASO/RNA duplex, which is expected to form an A-type duplex structure like DNA/RNA and RNA/RNA duplexes, a non-bridging oxygen atom of a phosphodiester linkage in the DNA strand is close to the 5-H atom/5-CH_3 group of pyrimidine nucleobases or to the 8-H atom of purine nucleobases in the DNA strand. Accordingly, in (*R*p)-PS modified DNA, the sulfur atom is close to the hydrogen atom or to the methyl group (Fig. 2),[13] whereas in (*S*p)-PS modified DNA, the non-bridging oxygen atom is close to the hydrogen atom or the methyl group. Therefore, the different location of the kind of non-bridging atoms is expected to affect the interactions between the non-bridging atoms and the nucleobase-derived substituents, as well as the properties of the nucleic acid duplexes.

Regarding the interactions between the non-bridging sulfur or oxygen atoms and nucleobases, C5-modified pyrimidine nucleobases have possibilities to exhibit discriminating features when combined with stereoregulated PS-DNAs. C5-Modified deoxyuridine derivatives have been studied to improve the properties of nucleic acids such as the affinity to their complementary RNAs and the nuclease resistance.[14–29] C5-Modified deoxycytidine derivatives have also been explored for similar purposes,[21,24,26] while 5-methyl cytosine has been used to inhibit immune responses derived from CpG sequences.[30,31] In this study, we focused on the combination of stereoregulated PS linkages and C-5 modified uracil nucleobases using 5-methyl deoxyuridine, known as thymidine, 5-bromo deoxyuridine (d^{Br}U), 5-iodo deoxyuridine (d^{I}U), and 5-propynyl deoxyuridine (d^{pr}U) units (Fig. 3). While the methyl, bromo and iodo substituents were expected to be close to one of the non-bridging atoms of a PS linkage in the duplex structure, the propynyl group in d^{pr}U was expected to be located close to two non-bridging atoms of two different internucleotide linkages, as shown in Fig. 4.[28]

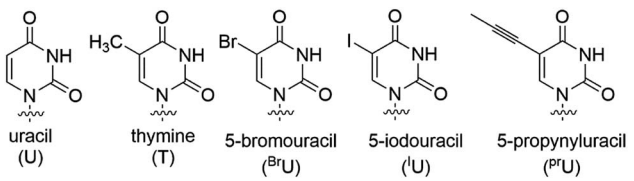

Fig. 3 5′-Modified (and unmodified) uracil bases used in this study.

In this study, DNA oligomers containing consecutive base sequences of these deoxyuridine derivatives, dCG(^{x}U$_{PS}$)$_8$CG (d^{x}U represents 5-modified or unmodified deoxyuridine), were designed and synthesized in a stereoregulated manner. The properties of these DNA oligomers including duplex forming ability and RNase H activity were also evaluated.

Results and discussion

Synthesis of stereopure PO/PS chimeric DNA oligomers containing C-5 modified deoxyuridine derivatives

Oxazaphospholidine monomer units were initially prepared for the synthesis of DNA oligomers with stereoregulated PS linkages by an oxazaphospholidine approach.[32–34] The thymidine monomers (***Rp***)- and (***Sp***)-**3b** were synthesized according to our previous report.[33] 5′-DMTr-protected dU (**1a**),[35] d^{Br}U (**1c**),[36] and d^{I}U (**1d**)[36] were prepared following already reported procedures, while 5′-DMTr-protected d^{Pr}U (**1e**) was synthesized from **1d** *via* the Sonogashira coupling.[37] **1a**, **1c**, **1d**, and **1e** were then used to prepare the corresponding oxazaphospholidine monomers (**3a**, **3c**, **3d**, and **3e**) by the conventional method.[33,38] All the *S*p- and *R*p monomers were synthesized in moderate yields with high stereopurities (Table 1).

Subsequently, ten DNA 12mers containing eight consecutive U or modified-U sequences (dCG(^{x}U$_{PS}$)$_8$CG) were synthesized based on the automated stereocontrolled solid-phase synthesis

Table 1 Synthesis of the oxazaphospholidine monomer units

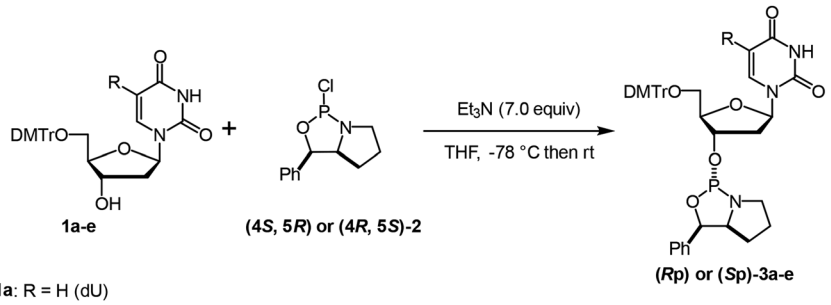

1a: R = H (dU)
1b: R = CH_3 (T)
1c: R = Br ($d^{Br}U$)
1d: R = I ($d^{I}U$)
1e: R = propynyl ($d^{pr}U$)

Entry	Compound	^{x}U	Yield (%)	dr[a] (*Rp* : *Sp*)	Purity[a] (%)
1	(*Rp*)-**3a**	U	45	>99 : 1	89
2	(*Rp*)-**3b**	T	60	>99 : 1	98
3	(*Rp*)-**3c**	^{Br}U	41	>99 : 1	97
4	(*Rp*)-**3d**	^{I}U	42	>99 : 1	97
5	(*Rp*)-**3e**	^{pr}U	42	>99 : 1	>99
6	(*Sp*)-**3a**	U	57	>1 : 99	95
7	(*Sp*)-**3b**	T	44	>1 : 99	>99
8	(*Sp*)-**3c**	^{Br}U	49	>1 : 99	99
9	(*Sp*)-**3d**	^{I}U	50	>1 : 99	96
10	(*Sp*)-**3e**	^{pr}U	53	>1 : 99	98

[a] Determined by ^{31}P NMR.

of (PO/PS) chimeric DNA oligomers (Fig. 5).[34] Eight PS modification sites were designed to all the *Rp* or *Sp* configurations in the respective DNA oligomers. For the synthesis of DNA containing halouracil derivatives ($d^{Br}U$ and $d^{I}U$), dC^{ac}-, and $dG^{ipr\text{-}pac}$-phosphoramidites and CPG-$dG^{ipr\text{-}pac}$ were used instead of dC^{bz}- and dG^{ibu}-phosphoramidites and CPG-dG^{ibu}, for deprotection under milder conditions in order to avoid 5-amination by ammonia.[39] All the DNA oligomers (***Rp***)- or (***Sp***)-**4a–4e** were successfully synthesized as shown in Table 2.

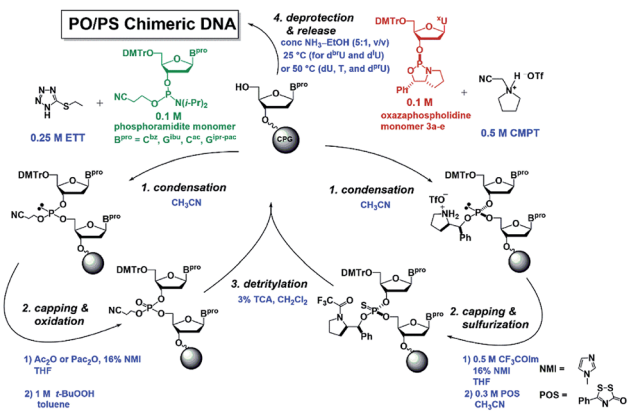

Fig. 5 Automated solid-phase synthesis of PO/PS chimeric DNA oligomers in a stereoregulated manner.

UV melting analysis

UV melting analysis was conducted to evaluate the duplex forming ability of the synthesized DNA oligomers. The UV melting curves of the DNA oligomers and their complementary 12mer RNA, $rCGA_8CG$, are depicted in Fig. 6, and the melting temperatures (T_m) are listed in Table 3. In all cases, the DNA/RNA hybrid duplexes of the (*Rp*)-PO/PS-DNA oligomers exhibited higher T_m values than those of the (*Sp*)-PS/PO-DNA oligomers. These results were consistent with previous reports and the differences in the properties between the two diastereomers.[7,8,11,34,40] Moreover, the ΔT_m values between the PO/(*Rp*)-PS-DNAs and the PO/(*Sp*)-PS-DNAs were different depending on the substituents on the C-5 position. In the case of $dCG(U_{PS})_8CG$ (**4a**) and $dCG(T_{PS})_8CG$ (**4b**), the ΔT_m values between the PO/(*Rp*)-PS-DNAs and PO/(*Sp*)-PS-DNAs were relatively small, 2.8 °C and 2.9 °C, respectively. The halogen modification also increased the ΔT_m values, with (*Rp*)- $dCG(^{Br}U_{PS})_8CG$/RNA and (*Rp*)-$dCG(^{I}U_{PS})_8CG$/RNA duplexes showing higher ΔT_m than their corresponding (*Sp*)-DNA/RNA duplexes by 5.1 and 5.7 °C, respectively. In the case of ^{Pr}U, the (*Rp*)-$dCG(^{Pr}U_{PS})_8CG$/RNA duplex showed a quite high T_m value (61.8 °C, (***Rp***)-**4e**) compared to the (*Sp*)-$dCG(^{Pr}U_{PS})_8CG$/RNA duplex (44.1 °C, (***Sp***)-**4e**), and its ΔT_m value was 17.7 °C. The T_m value was even higher than that of the corresponding PO-DNA/RNA duplex (60.3 °C), while in all other DNA oligomers, the T_m values of both (*Sp*)- and (*Rp*)-DNA/RNA duplexes were by more than 10 °C lower than

Table 2 Synthesis of the PO/PS chimeric DNA oligomers

Entry	Compound	Sequence and modification	CPG	Amidite monomer	Yield/%
1	**(*Rp*)-4a**	(*Rp*)-d(CG(U_{PS})$_8$CG)	dG^{ibu}	dG^{ibu}, dC^{bz}	20
2	**(*Sp*)-4a**	(*Sp*)-d(CG(U_{PS})$_8$CG)			28
3	**(*Rp*)-4b**	(*Rp*)-d(CG(T_{PS})$_8$CG)			19
4	**(*Sp*)-4b**	(*Sp*)-d(CG(T_{PS})$_8$CG)			24
5	**(*Rp*)-4c**	(*Rp*)-d(CG($^{Br}U_{PS}$)$_8$CG)	$dG^{ipr\text{-}pac}$	$dG^{ipr\text{-}pac}$, dC^{ac}	10
6	**(*Sp*)-4c**	(*Sp*)-d(CG($^{Br}U_{PS}$)$_8$CG)			2
7	**(*Rp*)-4d**	(*Rp*)-d(CG($^{I}U_{PS}$)$_8$CG)			2
8	**(*Sp*)-4d**	(*Sp*)-d(CG($^{I}U_{PS}$)$_8$CG)			6
9	**(*Rp*)-4e**	(*Rp*)-d(CG($^{pr}U_{PS}$)$_8$CG)	dG^{ibu}	dG^{ibu}, dC^{bz}	29
10	**(*Sp*)-4e**	(*Sp*)-d(CG($^{pr}U_{PS}$)$_8$CG)			5

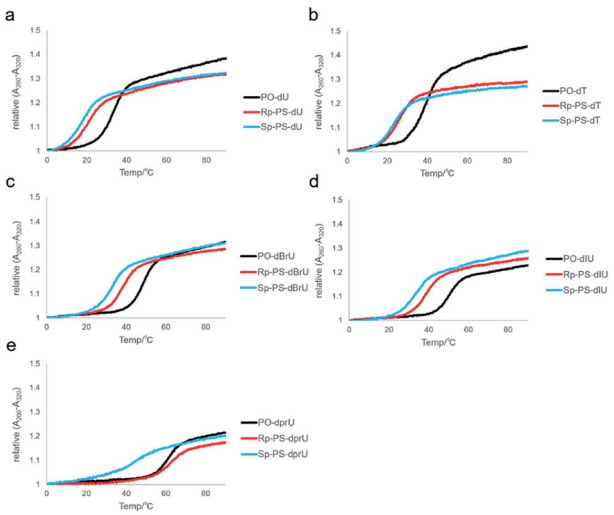

Fig. 6 UV melting curves of the hybrid duplex of dCG($^{X}U_{PS}$)$_8$CG or dCG($^{X}U_{PO}$)$_8$CG and rCGA$_8$CG. (a) $^{X}U = U$, (b) $^{X}U = T$, (c) $^{X}U = {}^{Br}U$, (d) $^{X}U = {}^{I}U$, and (e) $^{X}U = {}^{pr}U$.

Table 3 T_m values of the hybrid duplex of dCG($^{X}U_{PS}$)$_8$CG or dCG($^{X}U_{PO}$)$_8$CG and rCGA$_8$CG

Entry	^{X}U	PO or PS	Compound	T_m/°C	ΔT_m/°C (PS − PO)	ΔT_m/°C (*Rp* − *Sp*)
1	U	PO	—	32.7	—	2.8
2	U	(*Rp*)-PS	**(*Rp*)-4a**	20.6	−12.1	
3	U	(*Sp*)-PS	**(*Sp*)-4a**	17.8	−14.9	
4	T	PO	—	38.7	—	2.9
5	T	(*Rp*)-PS	**(*Rp*)-4b**	26.2	−12.5	
6	T	(*Sp*)-PS	**(*Sp*)-4b**	23.3	−15.4	
7	^{Br}U	PO	—	47.9	—	5.1
8	^{Br}U	(*Rp*)-PS	**(*Rp*)-4c**	37.8	−10.1	
9	^{Br}U	(*Sp*)-PS	**(*Sp*)-4c**	32.7	−15.2	
10	^{I}U	PO	—	49.9	—	5.7
11	^{I}U	(*Rp*)-PS	**(*Rp*)-4d**	37.9	−12.0	
12	^{I}U	(*Sp*)-PS	**(*Sp*)-4d**	32.2	−17.7	
13	^{pr}U	PO	—	60.3	—	17.7
14	^{pr}U	(*Rp*)-PS	**(*Rp*)-4e**	61.8	1.5	
15	^{pr}U	(*Sp*)-PS	**(*Sp*)-4e**	44.1	−16.2	

those of each PO-DNA/RNA duplex. These results suggested the existence of specific stabilization effects deriving from the combination of the (*Rp*)-PS linkage and the propynyl group of **(*Rp*)-4e**. In the **(*Rp*)-4e**/RNA duplex, each propynyl group is expected to be located close to two sulfur atoms of two consecutive (*Rp*)-PS-nucleotides (Fig. 4). The manners of interaction of the sulfur atom in a phosphorothioate linkage are different from those of the oxygen atom in many points;[41,42] electrostatic interactions, hydrogen bonding, hydrophobic interactions, and hydration. Since propynyl groups have no ability to form hydrogen bonds and electrostatically interact with other moieties, the stabilization in the case of **(*Rp*)-4e** might be derived from the hydrophobic interactions between the sulfur atoms in the PS linkages and the propynyl group.

UV melting analysis was also performed for the duplexes of the synthesized DNAs and their complementary DNA. The corresponding curves and T_m values of dCG($^{X}U_{PS}$)$_8$CG/dCGA$_8$CG are presented in Fig. 7 and Table 4. In the case of dCG(U_{PS})$_8$CG and dCG(T_{PS})$_8$CG, the T_m values of PO/(*Rp*)-PS-DNA/DNAs and PO/(*Sp*)-PS-DNA/DNAs were slightly different than those of DNA/RNAs. Even for dCG($^{Br}U_{PS}$)$_8$CG and dCG($^{I}U_{PS}$)$_8$CG (**4c** and

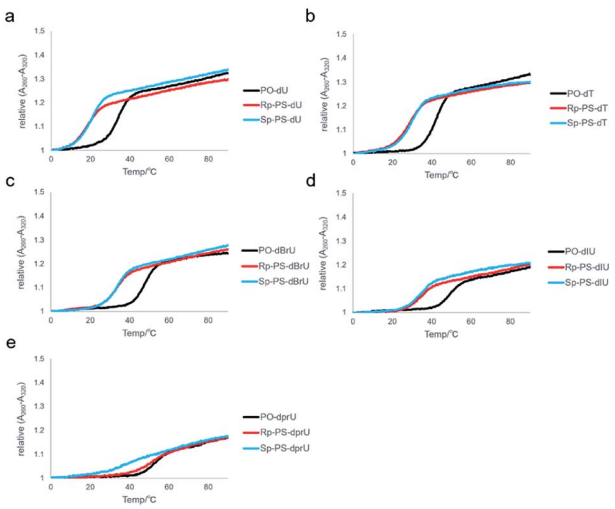

Fig. 7 UV melting curves of the duplex of dCG($^{X}U_{PS}$)$_8$CG or dCG($^{X}U_{PO}$)$_8$CG and dCGA$_8$CG. (a) $^{X}U = U$, (b) $^{X}U = T$, (c) $^{X}U = {}^{Br}U$, (d) $^{X}U = {}^{I}U$, and (e) $^{X}U = {}^{pr}U$.

Table 4 T_m values of the duplex of dCG($^{X}U_{PS}$)$_8$CG or dCG($^{X}U_{PO}$)$_8$CG and dCGA$_8$CG

Entry	^{X}U	PO or PS	Compound	T_m/°C	ΔT_m/°C (PO − PS)	ΔT_m/°C (*R*p − *S*p)
1	U	PO	—	33.5	—	−1.8
2	U	(*R*p)-PS	**(*R*p)-4a**	18.0	−15.5	
3	U	(*S*p)-PS	**(*S*p)-4a**	19.8	−13.7	
4	T	PO	—	41.4	—	−0.9
5	T	(*R*p)-PS	**(*R*p)-4b**	28.4	−13.0	
6	T	(*S*p)-PS	**(*S*p)-4b**	29.3	−12.1	
7	^{Br}U	PO	—	47.3	—	−0.4
8	^{Br}U	(*R*p)-PS	**(*R*p)-4c**	33.0	−14.3	
9	^{Br}U	(*S*p)-PS	**(*S*p)-4c**	33.4	−13.9	
10	^{I}U	PO	—	48.7	—	0.0
11	^{I}U	(*R*p)-PS	**(*R*p)-4d**	33.2	−15.5	
12	^{I}U	(*S*p)-PS	**(*S*p)-4d**	33.2	−15.5	
13	^{pr}U	PO	—	51.1	—	9.7
14	^{pr}U	(*R*p)-PS	**(*R*p)-4e**	50.1	−1.0	
15	^{pr}U	(*S*p)-PS	**(*S*p)-4e**	40.4	−10.7	

4d), almost no differences were observed in the T_m values of the two isomers. Only in the case of dCG($^{pr}U_{PS}$)$_8$CG (**4e**), the T_m value of (*R*p)-dCG($^{pr}U_{PS}$)$_8$CG/DNA was similar to that of the corresponding PO-DNA/DNA, and higher than that of the PO/(*S*p)-PS-DNA/DNA duplex by 9.7 °C. The observed tendency was similar to that indicated for the DNA/RNA hybrid duplexes, suggesting also a slightly lower stabilization effect deriving from the combination between (*R*p)-PS linkages and 5-propynyl groups in the DNA/DNA duplexes.

The difference in the T_m values between the two stereoisomers was lower in the DNA/DNA duplexes than in the DNA/RNA hybrid duplexes in all cases. It is possible to be due to their different duplex structures. The DNA/DNA duplexes adopt a B-type duplex structure, whereas the DNA/RNA duplexes basically form an A-type duplex. Additional variations have also been observed in several structural parameters,[43] which can be visually identified, as the A-type duplexes have a narrower and deeper major groove and a wider and shallower minor groove than B-type duplexes. These structural differences possibly affect the distance between atoms and substituents. Regarding the hydrophobic or other interactions between the substituents at the 5-position and the sulfur atom of the (*R*p)-PS linkage, the distance between the sulfur atom and the carbon, bromine, or iodine atom at the 5-position is expected to be longer in the DNA/DNA duplexes than in the DNA/RNA hybrids by about 1 Å (Fig. S38†),[44] possibly leading to the different duplex forming abilities.

Evaluation of RNase H activity

The RNase H activity of the stereoregulated PO/PS-chimeric DNA 12mers containing ^{pr}U bases was explored. For the evaluation experiments, **4b**, **4e**, and the corresponding PO-DNA oligomers were used. Each DNA and an excess amount of the 12mer complementary RNA were treated with *E. coli* RNase H at 20 °C for 30 min. Fig. 8b–g illustrate the HPLC profiles of each mixture after treatment with RNase H. It was previously reported that (*R*p)-PS rich DNAs show higher RNase H activity than (*S*p)-PS rich DNAs with respect to *E. coli* RNase H.[10] As shown in Fig. 8b and c,

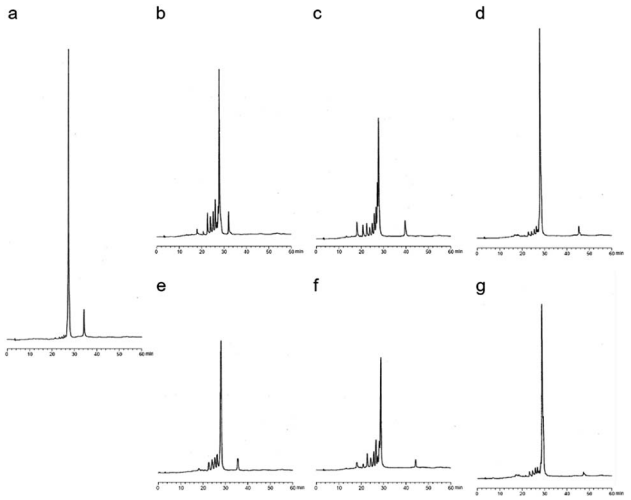

Fig. 8 (a) RP-HPLC of the mixture of dCG(^{pr}U)$_8$CG and the complementary RNA (rCGA$_8$CG) without RNase H treatment; (b)–(g) RP-HPLC profiles of the mixture of PO- or PO/PS chimeric-DNAs and their complementary RNA (rCGA$_8$CG) after treatment with 4 U/100 μL RNase H at 20 °C for 30 min: (b) PO-dCGT$_8$CG, (c) (*R*p)-dCG(T$_{PS}$)$_8$CG (**Rp-(4b)**), (d) (*S*p)-dCG(T$_{PS}$)$_8$CG (**Sp-(4b)**), (e) PO-dCG(^{pr}U)$_8$CG, (f) (*R*p)-dCG($^{pr}U_{PS}$)$_8$CG (**Rp-(4e)**), (g) (*S*p)-dCG($^{pr}U_{PS}$)$_8$CG (**Sp-(4e)**). The RP-HPLC analyses (UV detection at 260 nm) were performed with a linear gradient of 0–30% CH$_3$CN in 0.1 M triethyl ammonium acetate (TEAA) buffer (pH 7.0) at 20 °C for 60 min with a flow rate of 0.5 mL min^{-1}.

(*R*p)-4b had similar RNase H activity as PO-dCG(T$_{PS}$)$_8$CG. In contrast, only small peaks of cleaved RNA fragments were observed in the presence of **(*S*p)-4b** (Fig. 8d), complying with the previous results.[10] Furthermore, in the case of ^{pr}U, **(*R*p)-4e** showed high RNase H activity (Fig. 8f), similar to that of **(*R*p)-4b**. **(*S*p)-4e** also exhibited similar profiles to **(*S*p)-4b**, and only small amounts of RNA was cleaved (Fig. 8g). Additional reaction conditions with higher RNase H concentrations (Fig. S39†) were also applied, but no significant differences were detected in the RNase H activity by base modifications. Therefore, it was indicated that the propynyl modification combined with the (*R*p)-PS modification significantly increased the T_m values of the DNA/RNA hybrid duplexes without altering the RNase H activity.

Conclusions

This study revealed that the combination of the stereochemistry of PS linkages with C5-modifications of uracil bases on a DNA strand could strongly affect the thermal stability of DNA/RNA duplexes. In particular, the C5-propyny modification significantly increased the T_m value of a DNA/RNA hybrid duplex when combined with (*R*p)-PS linkages while maintaining the RNase H activity. These results would be useful for the design of ASOs and other nucleic acid drugs with stereopure PS linkages.

Experimental section

General information

All reactions were conducted under argon atmosphere. The ^{1}H NMR spectra were obtained at 400 MHz on a JEOL instrument

with tetramethylsilane as an internal standard (δ 0.0 ppm). The ^{13}C NMR spectra were obtained at 100 MHz with $CDCl_3$ as an internal standard (δ 77.0 ppm). The ^{31}P NMR spectra were obtained at 162 MHz with 85% H_3PO_4 as an external standard (δ 0.0 ppm). The PO-DNA and RNA oligomers were purchased from Japan Bio Services Co., LTD. Silica gel column chromatography was performed using silica gel 60 N (neutral silica) or Chromatorex NH-DM1020 (amino silica). Reverse phase (RP)-HPLC was performed for the analysis and purification of the synthesized analogs using a μBondasphere column (5 μm, C18, 100 Å, 3.9 × 150 mm) (Waters) or Source 5 RPC ST 4.6/150 (GE Healthcare). The organic solvents were dried before use. The mass spectra were recorded on a 910-MS FTMS system (Varian, ESI-MS) or a JMS-700 instrument (JEOL, FAB-MS). The nucleoside phosphoramidites (B^{pro} = C^{bz}, C^{ac}, G^{ibu}, and $G^{ipr\text{-}pac}$) and solid supports were purchased from Glen Research Co., Ltd.

Automated solid-phase synthesis

The DNA oligomers were synthesized using an NTS M2 DNA/RNA synthesizer (Nihon Techno Service Co., Ltd) based on the following procedure.

		Cycle for PO		Cycle for PS	
Step	Operation	Reagents	Time	Reagents	Time
1	Detritylation	3% (w/v) TCA in CH_2Cl_2	12 s	3% (w/v) TCA in CH_2Cl_2	12 s
2	Washing	Dry CH_3CN	—	Dry CH_3CN	—
3	Condensation	0.1 M phosphoramidite monomer and 0.25 M ETT in dry CH_3CN	30 s	0.1 M oxazaphospholidine monomer and 0.5 M CMPT in dry CH_3CN	10 min
4	Washing	Dry CH_3CN	—	Dry CH_3CN	—
5	Capping	Ac_2O or Pac_2O and 6% (v/v) NMI in dry THF	40 s	0.5 M CF_3COIm and 16% (v/v) NMI in dry THF	40 s
6	Washing	Dry CH_3CN	—	Dry CH_3CN	—
7	Oxidation/ sulfurization	1 M *t*-BuOOH in dry toluene	30 s	0.3 M POS in dry CH_3CN	8 min
8	Washing	Dry CH_3CN	—	Dry CH_3CN	—

After synthesis, each solid support was treated with a mixture of conc. NH_3(aq)–EtOH (5 : 1, v/v) at 50 °C for 8–12 h. In the case of oligomers containing ^{Br}U or ^{I}U bases (**4c** and **4d**), each solid support was treated with conc. NH_3(aq)–EtOH (5 : 1, v/v) at 25 °C for 13–24 h. Then, the mixture was filtered and the filtrate was concentrated. The crude product was purified by RP-HPLC to afford pure stereoregulated PS/PO-chimeric DNA oligomers. The synthesized DNA oligomers were quantified by their UV absorbance and predicted extinction coefficients at 260 nm,[19,45] except for **4e**. The quantification of **4e** was performed by the high temperature UV absorbance and predicted extinction coefficients at 280 nm.[23]

(*Rp*)-4a ((*Rp*)-dCG(U_{PS})$_8$CG). The automated solid-phase synthesis procedure was applied using 5′-*O*-DMTr-dG^{ibu}-CPG (0.5 μmol) as the solid support, **(*Sp*)-3a** as the oxazaphospholidine monomer, and dG^{ibu} and dC^{Bz} phosphoramidite monomers.

ESI-HRMS: *m*/*z* calcd for $C_{110}H_{132}N_{32}O_{70}P_{11}S_8^{5-}$ $[M - 5H]^{5-}$; 723.4532. Found; 723.4550.

(*Sp*)-4a ((*Sp*)-dCG(U_{PS})$_8$CG). The automated solid-phase synthesis procedure was applied using 5′-*O*-DMTr-dG^{ibu}-CPG (0.5 μmol) as the solid support, **(*Rp*)-3a** as the oxazaphospholidine monomer, and dG^{ibu} and dC^{Bz} phosphoramidite monomers.

ESI-HRMS: *m*/*z* calcd for $C_{110}H_{132}N_{32}O_{70}P_{11}S_8^{5-}$ $[M - 5H]^{5-}$; 723.4532. Found; 723.4547.

(*Rp*)-4b ((*Rp*)-dCG(T_{PS})$_8$CG). The automated solid-phase synthesis procedure was applied using 5′-*O*-DMTr-dG^{ibu}-CPG (0.5 μmol) as the solid support, **(*Sp*)-3b** as the oxazaphospholidine monomer, and dG^{ibu} and dC^{Bz} phosphoramidite monomers.

ESI-HRMS: *m*/*z* calcd for $C_{118}H_{148}N_{32}O_{70}P_{11}S_8^{5-}$ $[M - 5H]^{5-}$; 745.8782. Found; 745.8804.

(*Sp*)-4b ((*Sp*)-dCG(T_{PS})$_8$CG). The automated solid-phase synthesis procedure was applied using 5′-*O*-DMTr-dG^{ibu}-CPG (0.5 μmol) as the solid support, **(*Rp*)-3b** as the oxazaphospholidine monomer, and dG^{ibu} and dC^{bz} phosphoramidite monomers.

ESI-HRMS: *m*/*z* calcd for $C_{118}H_{148}N_{32}O_{70}P_{11}S_8^{5-}$ for $[M - 5H]^{5-}$; 745.8782. Found; 745.8792.

(*Rp*)-4c ((*Rp*)-dCG($^{Br}U_{PS}$)$_8$CG). The automated solid-phase synthesis procedure was applied using 5′-*O*-DMTr-$dG^{ipr\text{-}pac}$-CPG (0.5 μmol) as the solid support, **(*Sp*)-3c** as the oxazaphospholidine monomer, and $dG^{ipr\text{-}pac}$ and dC^{ac} phosphoramidite monomers.

ESI-HRMS: *m*/*z* calcd for $C_{110}H_{124}Br_8N_{32}O_{70}P_{11}S_8^{5-}$ $[M - 5H]^{5-}$; 850.1097. Found; 850.1099.

(*Sp*)-4c ((*Sp*)-dCG($^{Br}U_{PS}$)$_8$CG). The automated solid-phase synthesis procedure was applied using 5′-*O*-DMTr-$dG^{ipr\text{-}pac}$-CPG (0.5 μmol) as the solid support, **(*Rp*)-3c** as the oxazaphospholidine monomer, and $dG^{ipr\text{-}pac}$ and dC^{ac} phosphoramidite monomers.

ESI-HRMS: *m*/*z* calcd for $C_{110}H_{124}Br_8N_{32}O_{70}P_{11}S_8^{5-}$ $[M - 5H]^{5-}$; 850.1097. Found; 850.1089.

(*Rp*)-4d ((*Rp*)-dCG($^{I}U_{PS}$)$_8$CG). The automated solid-phase synthesis procedure was applied using 5′-*O*-DMTr-$dG^{ipr\text{-}pac}$-CPG (0.5 μmol) as the solid support, **(*Sp*)-3d** as the oxazaphospholidine monomer, and $dG^{ipr\text{-}pac}$ and dC^{ac} phosphoramidite monomers.

ESI-HRMS: *m*/*z* calcd for $C_{110}H_{124}I_8N_{32}O_{70}P_{11}S_8^{5-}$ $[M - 5H]^{5-}$; 924.8878. Found; 924.8895.

(*Sp*)-4d ((*Sp*)-dCG($^{I}U_{PS}$)$_8$CG). The automated solid-phase synthesis procedure was applied using 5′-*O*-DMTr-$dG^{ipr\text{-}pac}$-CPG (0.5 μmol) as the solid support, **(*Rp*)-3d** as the oxazaphospholidine monomer, and $dG^{ipr\text{-}pac}$ and dC^{ac} phosphoramidite monomers.

ESI-HRMS: *m*/*z* calcd for $C_{110}H_{124}I_8N_{32}O_{70}P_{11}S_8^{5-}$ $[M - 5H]^{5-}$; 924.8878. Found; 924.8882.

(*Rp*)-4e ((*Rp*)-dCG($^{pr}U_{PS}$)$_8$CG). The automated solid-phase synthesis procedure was applied using 5′-*O*-DMTr-dG^{ibu}-CPG (0.5 μmol) as the solid support, **(*Sp*)-3e** as the

oxazaphospholidine monomer, and dG^{ibu} and dC^{bz} phosphoramidite monomers.

ESI-HRMS: *m*/*z* calcd for $C_{134}H_{148}N_{32}O_{70}P_{11}S_8^{5-}$ $[M - 5H]^{5-}$; 784.2782. Found; 784.2794.

(*Sp*)-4e ((*Sp*)-dCG($^{pr}U_{PS}$)$_8$CG). The automated solid-phase synthesis procedure was applied using 5′-*O*-DMTr-dG^{ibu}-CPG (0.5 μmol) as the solid support, **(*Rp*)-3e** as the oxazaphospholidine monomer, and dG^{ibu} and dC^{bz} phosphoramidite monomers.

ESI-HRMS: *m*/*z* calcd for $C_{134}H_{148}N_{32}O_{70}P_{11}S_8^{5-}$ $[M - 5H]^{5-}$; 784.2782. Found; 784.2797.

UV melting analyses

The UV absorbance profiles over temperature were measured using an eight-sample cell changer in quartz cells of 1 cm path length. All the experiments were conducted in a 10 mM phosphate buffer containing 100 mM NaCl (pH 7.0), and the UV absorbance at 260 nm was monitored over temperature. Each sample containing 12mer DNA (2.5 μM) and its complementary oligonucleotide (DNA or RNA) was first rapidly heated to 95 °C, and, after 10 min, cooled to 0 °C at a rate of 0.5 °C min^{-1}. The dissociation process was recorded by heating to 95 °C at a rate of 0.5 °C min^{-1}.

RNase H assay

0.5 μM of 12mer DNA and 5 μM of the complementary RNA were dissolved in 10 mM Tris–HCl buffer containing 100 mM NaCl and 0.5 mM $MgCl_2$ (pH 7.5 at 20 °C). The solution was rapidly heated to 95 °C, and, after 10 min, cooled to 0 °C at a rate of 0.5 °C min^{-1}. 4 U or 20 U of RNase H was added to the solution (100 μL) and then the mixture was warmed to 20 °C. After 30 min, the mixture was rapidly heated to 95 °C, left for 1 min, and then rapidly cooled to 4 °C. The mixture was analyzed by RP-HPLC.

Conflicts of interest

The authors have no conflicts of interest to declare.

Acknowledgements

This work was supported by JSPS KAKENHI (Grant Number 15H03839).

Notes and references

1 S. T. Crooke, J. L. Witztum, C. F. Bennett and B. F. Baker, *Cell Metab.*, 2018, **27**, 714–739.
2 J. Kurreck, *Eur. J. Biochem.*, 2003, **270**, 1628–1644.
3 M. Nowotny, S. A. Gaidamakov, R. J. Crouch and W. Yang, *Cell*, 2005, **121**, 1005–1016.
4 M. Nowotny, S. A. Gaidamakov, R. Ghirlando, S. M. Cerritelli, R. J. Crouch and W. Yang, *Mol. Cell*, 2007, **28**, 264–276.
5 H. Inoue, Y. Hayase, S. Iwai and E. Ohtsuka, *FEBS Lett.*, 1987, **215**, 327–330.
6 W. Shen, C. L. D. Hoyos, M. T. Migawa, T. A. Vickers, H. Sun, A. Low, T. A. Bell, M. Rahdar, S. Mukhopadhyay, C. E. Hart, M. Bell, S. Riney, S. F. Murray, S. Greenlee, R. M. Crooke, X. Liang, P. P. Seth and S. T. Crooke, *Nat. Biotechnol.*, 2019, **37**, 640–650.
7 N. Iwamoto, D. C. D. Butler, N. Svrzikapa, S. Mohapatra, I. Zlatev, D. W. Y. Sah, Meena, S. M. Standley, G. Lu, L. H. Apponi, M. Frank-Kamenetsky, J. J. Zhang, C. Vargeese and G. L. Verdine, *Nat. Biotechnol.*, 2017, **35**, 845–851.
8 M. Boczkowska, P. Guga and W. J. Stec, *Biochemistry*, 2002, **41**, 12483–12487.
9 H. Jahns, M. Roos, J. Imig, F. Baumann, Y. Wang, R. Gilmour and J. Hall, *Nat. Commun.*, 2015, **6**, 6317.
10 D. Yu, E. R. Kandimalla, A. Roskey, Q. Zhao, L. Chen, J. Chen and S. Agrawal, *Bioorg. Med. Chem.*, 2000, **8**, 275–284.
11 W. B. Wan, M. T. Migawa, G. Vasquez, H. M. Murray, J. G. Nichols, H. Gaus, A. Berdeja, S. Lee, C. E. Hart, W. F. Lima, E. E. Swayze and P. P. Seth, *Nucleic Acids Res.*, 2014, **42**, 13456–13468.
12 M. Li, H. L. Lightfoot, F. Halloy, A. L. Malinowska, C. Berk, A. Behera, D. Schümperli and J. Hall, *Chem. Commun.*, 2016, **53**, 541–544.
13 M. Bachelin, G. Hessler, G. Kurz, J. G. Hacia, P. B. Dervan and H. Kessler, *Nat. Struct. Biol.*, 1998, **5**, 271–276.
14 M. A. Bonham, S. Brown, A. L. Boyd, P. H. Brown, D. A. Bruckenstein, J. C. Hanvey, S. A. Thomson, A. Pipe, F. Hassman, J. E. Bisi, B. C. Froehler, M. D. Matteucci, R. W. Wagner, S. A. Noble and L. E. Babiss, *Nucleic Acids Res.*, 1995, **23**, 1197–1203.
15 A. J. Gutierrez, M. D. Matteucci, D. Grant, S. Matsumura, R. W. Wagner and B. C. Froehler, *Biochemistry*, 1997, **36**, 743–748.
16 R. W. Wagner, M. D. Matteucci, J. G. Lewis, A. J. Gutierrez, C. Moulds and B. C. Froehler, *Science*, 1993, **260**, 1510–1513.
17 Y. S. Sanghvi, G. D. Hoke, S. M. Freier, M. C. Zounes, C. Gonzalez, L. Cummins, H. Sasmor and P. D. Cook, *Nucleic Acids Res.*, 1993, **21**, 3197–3203.
18 L. Ötvös, J. Sági, G. Sági and A. Szemz, *Nucleosides Nucleotides*, 1999, **18**, 1929–1933.
19 G. Becher, J. He and F. Seela, *Helv. Chim. Acta*, 2001, **84**, 1048–1065.
20 C. Moulds, J. G. Lewis, B. C. Froehler, D. Grant, T. Huang, J. F. Milligan, M. D. Matteucci and R. W. Wagner, *Biochemistry*, 1995, **34**, 5044–5053.
21 J. Sági, A. Szemzö, K. Ébinger, A. Szabolcs, G. Sági, É. Ruff and L. Ötvös, *Tetrahedron Lett.*, 1993, **34**, 2191–2194.
22 T. W. Barnes and D. H. Turner, *J. Am. Chem. Soc.*, 2001, **123**, 9186–9187.
23 T. W. Barnes and D. H. Turner, *J. Am. Chem. Soc.*, 2001, **123**, 4107–4118.
24 T. W. Barnes and D. H. Turner, *Biochemistry*, 2001, **40**, 12738–12745.
25 B. M. Znosko, T. W. Barnes, T. R. Krugh and D. H. Turner, *J. Am. Chem. Soc.*, 2003, **125**, 6090–6097.
26 B. C. Froehler, R. J. Jones, X. Cao and T. J. Terhorst, *Tetrahedron Lett.*, 1993, **34**, 1003–1006.

27 T. Kottysch, C. Ahlborn, F. Brotzel and C. Richert, *Chem.–Eur. J.*, 2004, **10**, 4017–4028.
28 J. I. Gyi, D. Gao, G. L. Conn, J. O. Trent, T. Brown and A. N. Lane, *Nucleic Acids Res.*, 2003, **31**, 2683–2693.
29 M. Terrazas and E. T. Kool, *Nucleic Acids Res.*, 2009, **37**, 346–353.
30 A. M. Krieg, *Nucleic Acid Ther.*, 2012, **22**, 77–89.
31 G. F. Deleavey and M. J. Damha, *Chem. Biol.*, 2012, **19**, 937–954.
32 N. Oka, T. Wada and K. Saigo, *J. Am. Chem. Soc.*, 2003, **125**, 8307–8317.
33 N. Oka, M. Yamamoto, T. Sato and T. Wada, *J. Am. Chem. Soc.*, 2008, **130**, 16031–16037.
34 Y. Nukaga, N. Oka and T. Wada, *J. Org. Chem.*, 2016, **81**, 2753–2762.
35 D. M. Noll, A. M. Noronha and P. S. Miller, *J. Am. Chem. Soc.*, 2001, **123**, 3405–3411.
36 A. S. Hansen, A. Thalhammer, A. H. El-Sagheer, T. Brown and C. J. Schofield, *Bioorg. Med. Chem. Lett.*, 2011, **21**, 1181–1184.
37 D. A. Berry, K.-Y. Jung, D. S. Wise, A. D. Sercel, W. H. Pearson, H. Mackie, J. B. Randolph and R. L. Somers, *Tetrahedron Lett.*, 2004, **45**, 2457–2461.
38 W. B. Wan, M. T. Migawa, G. Vasques, H. M. Murray, J. G. Nichols, H. Gaus, A. Berdeja, S. Lee, C. E. Hart, W. F. Lima, E. E. Swayze and P. P. Seth, *Nucleic Acids Res.*, 2014, **42**, 13456–13468.
39 E. Ferrer, M. Wiersma, B. Kazimierczak, C. W. Müller and R. Eritja, *Bioconjugate Chem.*, 1997, **8**, 757–761.
40 M. E. Østergaard, C. L. De Hoyos, W. B. Wan, W. Shen, A. Low, A. Berdeja, G. Vasquez, S. Murray, M. T. Migawa, X. Liang, E. E. Swayze, S. T. Crooke and P. P. Seth, *Nucleic Acids Res.*, 2020, **48**, 1691–1700.
41 P. A. Frey and R. D. Sammons, *Science*, 1985, **228**, 541–545.
42 D. Dertinger, L. S. Behlen and O. C. Uhlenbeck, *Biochemistry*, 2000, **39**, 55–63.
43 T. E. Cheatham and P. A. Kollman, *J. Am. Chem. Soc.*, 1997, **119**, 4805–4825.
44 A. Ghosh, R. K. Kar, J. Jana, A. Saha, B. Jana, J. Krishnamoorthy, D. Kumar, S. Ghosh, S. Chatterjee and A. Bhunia, *ChemMedChem*, 2014, **9**, 2052–2058.
45 W. M. Flanagan and R. W. Wagner, *Mol. Cell. Biochem.*, 1997, **172**, 213–225.